Pseudoamorphization of Cs_2HgBr_4

D. Machon,[1,2] V. P. Dmitriev,[1] P. Bouvier,[2] P. N. Timonin,[3] V. B. Shirokov,[3] and H.-P. Weber[1,4]
[1]*Group "Structure of Material under Extreme Conditions" SNBL/ESRF, Boite Postale 220, 38043 Grenoble Cedex, France*
[2]*LEPMI, INPG-CNRS, 1130 rue de la Piscine, Boite Postale 75, 38402 St. Martin d'Hères Cedex, France*
[3]*Institute of Physics at Rostov State University, pr. Stachki 194, 344090 Rostov-on-Don, Russia*
[4]*Institute of Crystallography, University of Lausanne, CH-1015 Lausanne, Switzerland*
(Received 9 April 2003; revised manuscript received 2 July 2003; published 8 October 2003)

Synchrotron-radiation diffraction experiments have revealed the critical role of nonhydrostatic stresses in the pressure-induced long-range order dissipation in Cs_2HgBr_4 crystals. With nonhydrostatic loading, the samples lose, reversibly, long-range order on the scale observable with x-ray diffraction above 11 GPa while hydrostatic conditions preserve long-range order up to 40 GPa, the limit achieved experimentally. The phenomenon is interpreted in terms of inhomogeneous lattice deformations induced in the sample by deviatoric stresses. Diffraction patterns of synthetic grains with chaotic distribution of deformations were computed, which displayed a sufficiently good agreement between calculated and observed diffraction patterns as to support the model.

DOI: 10.1103/PhysRevB.68.144104 PACS number(s): 61.10.−i, 62.50.+p, 71.55.Jv

I. INTRODUCTION

Fundamental questions on the relationship between the glassy state as quenched from melt and the amorphous state as obtained in crystalline solids by applying pressure were raised along with the discovery of pressure-induced solid-state amorphization (PIA).[1] First explanations of the PIA effect were based on the structural analogy with rapidly frozen liquid, devoid of a long-range order; this seemed justified by the visual similarity of their diffraction patterns. Thus, solid-state amorphization process was considered as *metastable melting*, i.e., a structural disordering typical of the melting process, but kinetically hindered because of low temperature (see, for example, review papers[2–4]). This order of events was included in models used in first-principle calculations which verified the existence of an energy minimum, at high pressure, for the corresponding state. However, as more and more compounds were shown to exhibit PIA, and as the diversity of experimental techniques used to characterize the PIA state grew, a clearer understanding of the effect emerged. Although loss of long-range order was apparently a common characteristic, the driving forces behind the effect, the mechanisms of transformation, and the stability conditions for the ''amorphous'' phases seem to vary considerably from one compound to the next.

Amorphization can arise from genuine structural disorder on the atomic scale (*crystallographic disorder*) or from other causes such as decomposition of the initial compounds as well. In the case of crystallographic disorder we are dealing with a genuine loss in long-range order, due to disorder in the crystal structure at the atomic scale. This disordering may be both orientational and positional, but with only slight displacements on the atoms, no diffusion and no deviations from the initial chemical composition. The final disordered isotropic state is to be considered as a new phase, either stable or metastable. Precisely this latter process could be characterized as metastable melting. The onset of an intermediate, noncrystalline state between two crystal phases (due to a kinetically impeded structural phase transition) can also be considered, formally and under special conditions, as a crystallographic process.

A second mechanism of PIA is the *decomposition* of an initially structurally complex crystal into simpler components, most of them well crystallized, although of small particle size. The *first step* in chemical decomposition is incipient segregation. This frustrated state is similar to crystallographically disordered amorphous but is not a new thermodynamic state of the *original* crystal.

Although one can find numerous examples of the above mechanisms, there are many cases where neither one fits very well. This paper is about specific features of the pressure-induced amorphization process in Cs_2HgBr_4; it presents a model for the suppression of long-range order, namely, nonhomogeneous crystal lattice distortion. Such inhomogeneous distortions may have several origins. They may arise from a pressure-induced elastic lattice instability or they could be caused by the application of nonhydrostatic pressure on the powder particles. In the latter case, in particular for soft materials, the random deformations can be quite large and cause a drastic deformation of the crystal structure, similar to that occurring in a true thermodynamic transition to an amorphous phase. Only in the case of crystallographic disorder the long-range order within one crystallite is truly lost and ''amorphization'' is the proper term for transformation process; this is why we use the term pseudoamorphization to describe the state attained by Cs_2HgBr_4 when pressurized as powder under nonhydrostatic conditions.

II. EXPERIMENTAL

Cesium mercury tetrabromide, Cs_2HgBr_4, is known to crystallize at ambient conditions in the orthorhombic β-K_2SO_4-type structure (space group *Pnma*) with lattice parameters $a=10.248$ Å, $b=7.927$ Å, $c=13.901$ Å, showing a pseudohexagonal arrangement of the $HgBr_4$ tetrahedra.[5]

The present structural study of Cs_2HgBr_4 was carried out on single-crystalline plates with approximate dimensions 50 $\times 20 \times 50$ μm^3, cut perpendicular to **b** axis, and on powdered samples obtained by grinding the single crystals. Synchrotron-radiation measurements were performed at the Swiss-Norwegian (BM1A) and high-pressure (ID30) beam lines at the European Synchrotron Radiation Facility (ESRF, Grenoble, France) by angle-dispersive diffraction techniques using monochromatic radiation ($\lambda = 0.7000$ Å or $\lambda = 0.3738$ Å). In the ID30 setup a focused beam was collimated with a pin hole to a diameter of 25 μm while SNBL (BM1A) provided a nonfocused beam slit-collimated down to 60×60 μm^2. The two-dimensional diffraction images obtained with a MAR345 image plate detector were analyzed using the ESRF FIT2D software, yielding intensity vs 2θ patterns.[6] Diffraction patterns were measured in the range from 0° to 30°; this window was imposed by the exit slit of the diamond anvil cell.

The samples were loaded into gasketed diamond anvil cells with the 150 μm diameter hole of the stainless steel gasket preindented to a thickness 60–80 μm. Pressure was calibrated using the ruby fluorescence technique.[7] Measurements were carried out at room temperature in the pressure range up to 40.0 GPa.

In order to study the effect of hydrostaticity on the phase transformations, nonhydrostatic experiments (without pressure transmitting medium) were followed by measurements using (i) paraffin oil (nujol) which is known to stiffen into a rigid solid around 2.5 GPa at room temperature (so quasihydrostatic conditions are provided up to ~8 GPa) and (ii) liquid nitrogen which crystallizes to its β modification at 2.4 GPa and transforms into its δ phase at 4.8 GPa. Nevertheless, these crystalline phases are quite soft and provide good hydrostatic conditions. However at 16.5 GPa, with the appearance of a harder ε-N_2, a quasihydrostatic regime sets in.

III. EXPERIMENTAL RESULTS

A. Low-pressure crystal-crystal transformations

In earlier studies the *P-T* phase diagram of Cs_2HgBr_4 was studied only up to 0.5 GPa and in the temperature range 230–270 K by optical birefringence and ultrasonic techniques[8] (Fig. 1). With increasing pressure, Cs_2HgBr_4 was found to undergo a proper ferroelastic transition from its ambient orthorhombic form to a monoclinic one. This latter phase is likely to be the same as the "lock-in" $P2_1/n$ phase, observed at ambient pressure below $T = 234$ K.[5] According to Ref. 5, an incommensurate structure with the modulation vector $\mathbf{k}_0 = \delta_1 \mathbf{a}^*$, where $\delta_1 \simeq 0.15$ at $T = T_i$, is stable in Cs_2HgBr_4 at ambient pressure between $T_i = 234$ K and $T_c = 243$ K. The stability domain of this phase vanishes with increasing pressure and temperature, ending in a polycritical triple point at $P_c = 0.14$ GPa and $T_c = 253$ K (Fig. 1).[8] Our powder and single-crystal diffraction data do not confirm the latter results in their entirety.

Figure 2 shows selected powder-diffraction patterns obtained under quasihydrostatic conditions.[9] The data collected at nearly ambient pressure ($P = 0.5$ GPa) agree perfectly

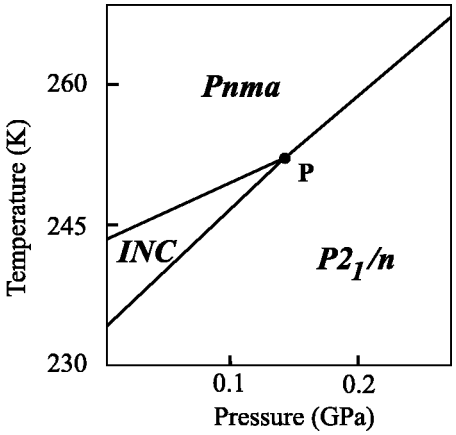

FIG. 1. Partial phase diagram of Cs_2HgBr_4 crystal (Ref. 8). P is the polycritical triple point.

with the previously reported orthorhombic structure[5]. The second-order Birch-Murnaghan equation of state

$$P = \frac{3}{2} K_{0T} \left[\left(\frac{V_0}{V} \right)^{7/3} - \left(\frac{V_0}{V} \right)^{3/2} \right], \tag{1}$$

fitted to data collected in the stability range of the orthorhombic phase (Fig. 3), yields the bulk modulus value $K_{0T}^{BM} = 6.1$ GPa (K'_{0T} was fixed at the value 4, $V_0 = 1129.7$ Å^3) that has the same order of magnitude as the one $K_{0T}^{ac} = 10.1$ GPa calculated using ultrasonic velocity data.[10] The notable difference in the bulk modulus values can be attributed to a truncated form of the equation of state (1) used in the fitting procedure. This limitation, in turn, results from the small number of experimental points obtained in the narrow stability range of the orthorhombic phase.

At $P \sim 1.2$ GPa onset of only weak new peaks and slight splittings of the existing ones indicate that Cs_2HgBr_4 undergoes a phase transition to a new phase only slightly distorted with respect to the orthorhombic parent one. The character of the distortion reveals itself in diffraction from single crystals. Figure 4 shows the evolution of the single-crystal diffraction patterns of Cs_2HgBr_4 over a wide pressure range, and under

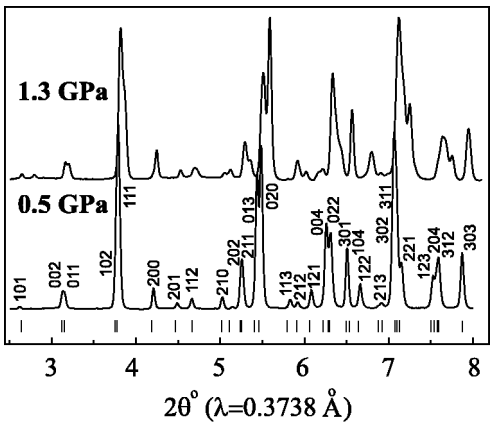

FIG. 2. Selected synchrotron-radiation powder-diffraction patterns of Cs_2HgBr_4 loaded with paraffin oil. The tick marks indicate the positions of calculated Bragg reflections in the orthorhombic phase.

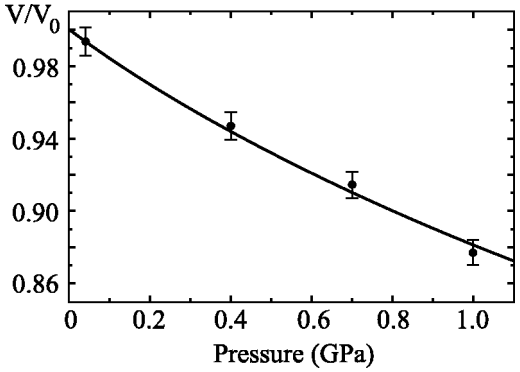

FIG. 3. Reduced volume V/V_0 plotted vs pressure for the orthorhombic phase of single-crystalline Cs_2HgBr_4. Line is the best fit to the second-order Birch-Murnaghan equation (1).

the same quasihydrostatic conditions as for the powder. At $P_i = 1.2$ GPa multiple superstructure reflections appear between Bragg spots. They can be indexed with $[k0l + \delta_2]$, where δ_2 is nonintegral. One can suggest that an incommensurate undulation with a wave vector $\mathbf{k}_0 = \delta_2 \mathbf{c}^*$ distorts the orthorhombic parent structure. At $P_l = 10.3$ GPa, well outside the pressure region where the pressure-transmitting medium is hydrostatic, this incommensurate perturbation locks into a structure, the diffraction patterns of which fit to a monoclinic phase with lattice parameters $a = 9.2$ Å, $b = 6.25$ Å, $c = 10.95$ Å, $\beta = 90.5°$, at 15.1 GPa. The experimental setup does not allow us to determine the crystal structure of this incommensurate phase with greater details, and this phase ought to be the subject of another study. However, from a comparison of Figs. 4(a) and 4(c) one can conclude that the two above phase transitions do not break single-crystalline form of the sample. Since the commensurate-to-incommensurate transition at $P_i = 1.2$ GPa, in a good agreement with a general theoretical conception, is continuous, this indicates that only *small spontaneous strains* are induced by the ferroelastic lock-in transformation at $P_l = 10.3$ GPa. We believe therefore that the observed transformations are of little relevance to the following amorphization as a *large* value of *deformation* is an inherent feature of the latter process.

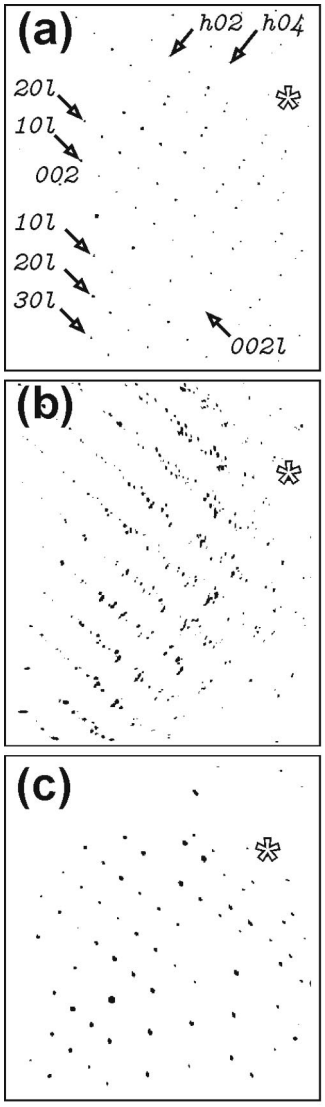

FIG. 4. Representative diffraction patterns ($\lambda = 0.3738$ Å) from single-crystalline Cs_2HgBr_4 at different pressures (nujol as pressure transmitting medium): (a) $P = 0.3$ GPa, (b) $P = 6.4$ GPa, (c) $P = 11.7$ GPa. Asterisks mark the diffraction spots due to dimond anvils.

B. High-pressure transformation of Cs_2HgBr_4

Although it is actually apparent that the details and even the occurrence of the amorphization process are sensitive to the state of stress undergone by the samples (hydrostatic versus nonhydrostatic loading), the precise role of nonhydrostatic stress components is not clear. Our work shows that certain data provide an important information on the amorphization mechanism.

Figure 5(a) displays powder-diffraction patterns of Cs_2HgBr_4 observed at various pressures under *nonhydrostatic* conditions, during compression. As pressure increases, one observes both peak broadening and a remarkable peak shift due to the large compressibility of the compound. Above 11 GPa, the broad peaks merge into haloes, which resemble those commonly observed in amorphous solids and liquids. In Cs_2HgBr_4 pressure thus induces a dissipation of the long-range order of the crystalline state.

In order to investigate the reversibility of the amorphization process, the diffraction pattern was also measured with decreasing pressure, as shown in Fig. 6. The haloes shift systematically towards lower angles, indicating a decrease in density. The halo pattern persists until pressure is released to almost atmospheric pressure (0.3 GPa) where a sudden recrystallization takes place (Fig. 6). The recrystallized product is a mixture of the parent orthorhombic structure and of the monoclinic phase. The halo patterns were reproducibly observed (see the second compression cycle in Fig. 6) and the recovered sample was invariably a two-phase mixture.

Solid-state amorphization in Cs_2HgBr_4 could be expected since it was predicted earlier on the basis of a "size criterion."[11] According to this simple rule molecular com-

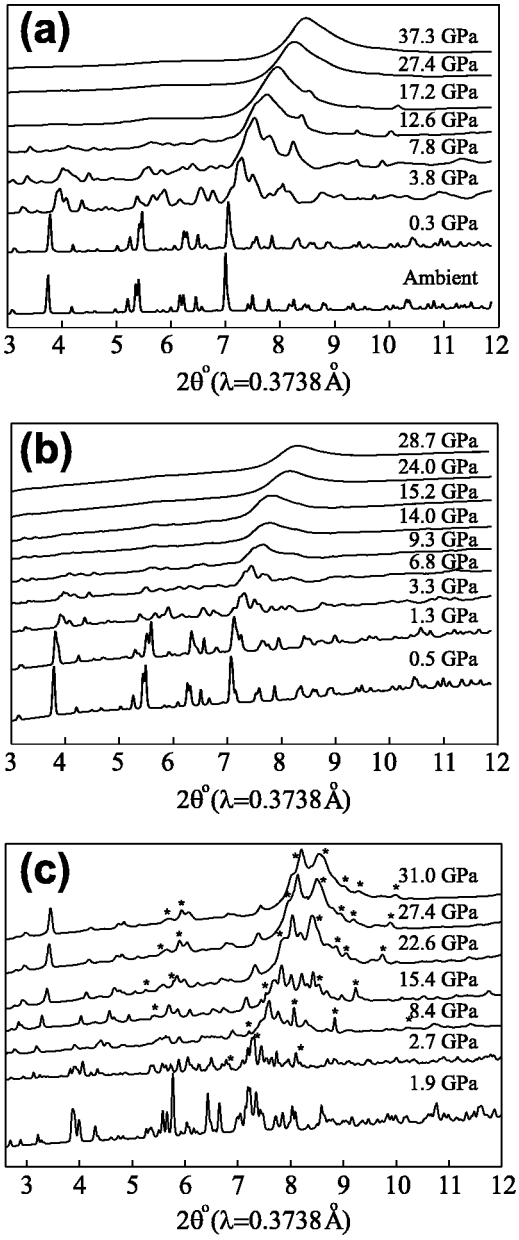

FIG. 5. Pressure evolution of powder-diffraction pattern of Cs_2HgBr_4 as a function of hydrostaticity in the first compression cycle. (a) Nonhydrostatic conditions (no pressure-transmitting medium); (b) in paraffin oil; (c) in nitrogen. Asterisks in (c) denote N_2 crystalline peaks.

pounds of the type A_2BX_4 amorphize if the $(r_B+r_X)/r_A$ anion/cation size ratio exceeds the threshold value of about 1.45. This is the case for Cs_2HgBr_4 where it equals 1.563.[11] Although, at the first sight, our experimental observations are consistent with this rule, the example at hand may well fall outside its range of applicability, as it presupposes crystallographic disordering in a hydrostatic sample environment.

Figures 5(b) and 5(c) show the changes in the diffraction pattern of Cs_2HgBr_4 with increasing hydrostaticity of the sample environment. With paraffin oil as pressure-transmitting medium, amorphization sets in at about its freezing pressure; the peaks broaden and eventually merge into haloes [Fig. 5(b)]. With N_2 as pressure-transmitting medium, there is no sign of amorphization until the gas has fully crystallized and its nonhydrostatic stress components come into play, producing amorphization of sample [Fig. 5(c)]. However, even at 30 GPa, the sample is far from the state which could be characterized as ''glass-like.'' It is important to note that all transformations both in quasihydrostatic and in hydrostatic conditions are reversible. We conclude that nonhydrostatic stresses with their corresponding pressure gradients promote an effect in Cs_2HgBr_4 that resembles dissipation of long-range order. A similar effect was reported, for example, in quartz[12] where improved hydrostaticity prevented the Bragg peaks from broadening, revealing in the process a two-phase mixture of a new monoclinic phase and Quartz II instead of the previously reported amorphous state.

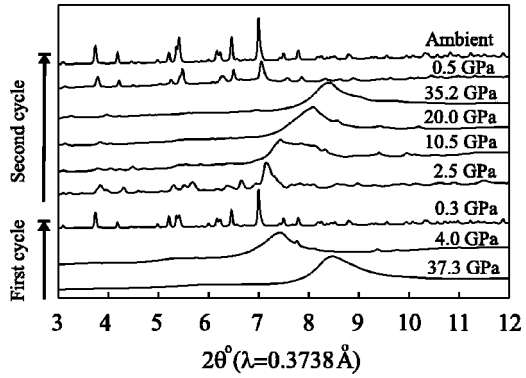

FIG. 6. Reversible pressure evolution of the powder-diffraction patterns of Cs_2HgBr_4 under nonhydrostatic conditions (from bottom to top). The first cycle continues the process presented in Fig. 5(a).

An important indication of the role of the mesoscopic state of a sample is provided by the experiment, discussed above, when a single-crystalline plate was immersed in paraffin oil. In variance with similar quasihydrostatic loading of powdered Cs_2HgBr_4 [Fig. 5(b)], single-crystalline sample compressed up to 13 GPa (maximal pressure achieved in the corresponding experiment) demonstrates slightly broadened well-shaped Bragg spots [Fig. 4(c)]. This observation seems to be a good demonstration of the importance, for the PIA effect in Cs_2HgBr_4, of both a granular sample form and the existence of pressure gradients and deviatoric stresses in the pressure chamber.

The other important detail in the Cs_2HgBr_4 pressure-induced conversion is its homogeneous character. One can see in Fig. 5 that broadening of diffraction peaks and their mergence into diffuse haloes occurs without arising of a glass-like background. Such a background would be typical for the heterogeneous nucleation of a new phase and is intrinsic for the chemical decomposition scenario of amorphization when, in a two-phase coexistence pressure range, the decrease of intensity of the broaden crystalline peaks occurs along with the increase of amorphous background (see, for example, observation in Ref. 13).

IV. MODEL

In the case of well-crystallized samples, diffraction methods provide the most detailed information on the structural

transformation mechanisms operative. Unfortunately, in the case of amorphization, poor quality of the diffraction spectra is inherent to the effect to be analyzed, and the structural information to be retrieved from the spectra is of no great import. Fortunately, other, nondiffraction evidences are available. For example, fast recovery of long-range order after pressure release (reversibility) is incompatible with the mechanism of chemical decomposition, particularly at low temperature. Also, if a nucleation stage, a characteristic intrinsic to diffusion-controlled solid-state reactions, is absent, chemical decomposition is again not the operative mechanism. However, if amorphization occurs irrespective of whether the pressure environment was hydrostatic or not, this is a good indication that decomposition is at work (see, for example, Ref. 13).

The reversibility of the amorphization process observed in Cs_2HgBr_4 as well as the lack of a nucleation stage also speaks against the crystallographic mechanism. In particular, elastic instability, which as a potential mechanism for amorphization requires the existence of off-diagonal (nonhydrostatic) components in the stress tensor, also calls for the existence of a *strongly first-order* structural phase transition prior to amorphization,[14–16] and such a transition is not observed in Cs_2HgBr_4, at least not in the pressure range that we studied.

In the following we will propose a mechanism for amorphization, one which accounts well for most, if not all, the diffraction features observed in Cs_2HgBr_4, such as line broadening and their merging in haloes, lack of glass-like background, and so forth.

In this model, the pressure-induced pseudoamorphous state is considered as a *randomly deformed crystal*, consisting of nearly homogeneous crystalline regions, subject to random deformations. This random mesoscopic structure is quite similar to the structural glass state appearing at phase transitions of crystals with compositional disorder.[17] It only differs by the size of the random deformations; in structural glasses, spontaneous deformations are much smaller. As diffraction is one of the principal tools to characterize the amorphization process we will show in this section the validity of the model by simulating the corresponding diffraction patterns.

Theoretical descriptions of the strength and distribution of random pressure-induced deformations are currently lacking; it is nevertheless possible to describe the x-ray and neutron scattering in such pseudoamorphous phases in a phenomenological way, assuming a chaotic distribution of the positions and deformations of different, nearly crystalline regions. One neglects the interference effects between the beams scattered by different crystallites and simply sum up their intensities. This is equivalent to the usual averaging of the scattering intensity of the (deformed) crystal over random deformations. Phenomenological Gaussian distribution function for random deformations has been developed for the diffraction in structural glass phases,[17] and it can also be applied, as we will now show, to the pressure-induced pseudoamorphous state, as long as one takes into account the large values of deformations in this case.

In the following we summarize the main features of our model. According to Ref. 17 we have for the average scattering intensity at transferred wave vector $\mathbf{Q}$

$$J(\mathbf{Q}) \approx N_d |F(\mathbf{Q})|^2 G(\mathbf{Q}),$$

$$F(\mathbf{Q}) = \sum_S f_S(\mathbf{Q}) \exp\{i\mathbf{Q}\mathbf{u}_S - W_S(\mathbf{Q})\},$$

$$2W_S(\mathbf{Q}) = \langle (\mathbf{Q}\tilde{\mathbf{u}}_S) \rangle_T,$$

$$G(\mathbf{Q}) = \left\langle \sum_n \exp[i\mathbf{Q}\mathbf{R}_n] \right\rangle_{\hat{e}}. \tag{2}$$

Here $\mathbf{R}_n$ are vectors of the center of mass of unit cells in deformed crystal,

$$\mathbf{R}_n = \mathbf{R}_n^0 + \hat{e}\mathbf{R}_n^0,$$

$\mathbf{R}_n^0$ being the corresponding vectors in original lattice and $\hat{e}$ is the tensor of random deformations. N_d is a number of quasicrystalline regions. We have the ordinary expressions for structural factors $F(\mathbf{Q})$ via atomic form-factors $f_S(\mathbf{Q})$ and vectors $\mathbf{u}_S$, defining atomic positions in unit cell, as well as the ordinary expressions for the Debye-Waller factors $W_S(\mathbf{Q})$. We consider them as referring to the original crystal lattice because the effect of random deformations on these quantities is negligible as compared to the effect of the shift of the cells positions.

The simplest supposition on the distribution function of random deformations is that it is Gaussian with zero mean $\langle e_{ij} \rangle = 0$ (as we can include nonzero $\langle e_{ij} \rangle$ in the definition of $\mathbf{R}_n^0$) and mean-square tensor of the general form $\langle e_{ij} e_{kl} \rangle = D_{ij,kl}$.

For this distribution $G(\mathbf{Q})$ becomes

$$G(\mathbf{Q}) = \sum_n \exp\{i\mathbf{Q}\mathbf{R}_n^0 - \langle (\mathbf{Q}\hat{e}\mathbf{R}_n^0)^2 \rangle / 2\}. \tag{3}$$

Considering large random deformations, we can neglect smearing of the spectrum due to the finiteness of quasicrystalline regions and assume that summation in Eq. (3) is over infinite lattice. Then $G(\mathbf{Q})$ can be transformed into (infinite) sum over reciprocal lattice vectors $\mathbf{B}$ of the original crystal,

$$G(\mathbf{Q}) = \frac{(2\pi)^{3/2}}{v_0 \sqrt{\det \hat{S}(\mathbf{Q})}} \times \sum_{\mathbf{B}} \exp\left\{ -\frac{1}{2} (\mathbf{Q}-\mathbf{B}) \hat{S}^{-1}(\mathbf{Q}) (\mathbf{Q}-\mathbf{B}) \right\}. \tag{4}$$

$$S_{i,j}(\mathbf{Q}) = D_{ij,kl} Q_k Q_l, \tag{5}$$

v_0 is unit cell volume.

Equations (2), (4), and (5) define the scattering intensity in pseudoamorphous phase, which is considered as a single crystal trapped in randomly deformed state. Each member of the sum in Eq. (4) represents broadened Bragg peak with the widths defined by the eigenvalues of matrix $S_{i,j}$ which grow as Q^2 at large Q.

One should choose only the form of the mean-square deformation tensor $D_{ij,kl} = \langle e_{ij} e_{kl} \rangle$ to make quantitative esti-

mations. The present state of theory does not allow one to make some definite predictions about the form of this tensor relative to the original crystal structure and the geometry of applied pressure. So, to compare qualitatively the predictions of Eqs. (2), (4), and (5), we assume in the following that in case of hydrostatic pressure $D_{ij,kl}$ have the simplest isotropic form,

$$D_{ij,kl}=DL^2\delta_{ij}\delta_{kl}+DT^2(\delta_{il}\delta_{jk}+\delta_{ik}\delta_{jl}-2\delta_{ij}\delta_{kl}). \quad (6)$$

Here $DL^2=\langle e_{xx}^2\rangle=\langle e_{yy}^2\rangle=\langle e_{zz}^2\rangle$, $DT^2=\langle e_{xy}^2\rangle=\langle e_{xz}^2\rangle=\langle e_{yz}^2\rangle$. Then

$$\hat{S}_{i,j}^{-1}(\mathbf{Q})=DL^{-2}Q^{-4}Q_iQ_j+DT^{-2}Q^{-4}(\delta_{ij}Q^2-Q_iQ_j),$$

$$\det\hat{S}(\mathbf{Q})=DL^2DT^4Q^6,$$

$$\frac{1}{2}(\mathbf{Q}-\mathbf{B})\hat{S}^{-1}(\mathbf{Q})(\mathbf{Q}-\mathbf{B})=\frac{1}{2DL^2}\left(1-\frac{\mathbf{QB}}{Q^2}\right)^2+\frac{1}{2DT^2}\left(\frac{B^2}{Q^2}-\frac{(\mathbf{QB})^2}{Q^4}\right). \quad (7)$$

Here we may note that we can also obtain the scattering intensity for powder diffraction by integrating the obtained single crystal intensity, Eqs. (2), (4), and (5), over directions of **Q**. In case of isotropic $D_{ij,kl}$ (6) one can obtain the approximate analytical expression for powder-diffraction intensity. To do this we note that only values of $F(\mathbf{Q})$ at $\mathbf{Q}=\mathbf{B}$ are relevant in the only interesting case when definite peaks exist. So we can write approximately

$$J(\mathbf{Q})=\frac{(2\pi)^{3/2}N_d}{v_0\sqrt{\det\hat{S}(\mathbf{Q})}}\sum_{\mathbf{B}}|F(\mathbf{B})|^2\times\exp\left\{-\frac{1}{2}(\mathbf{Q}-\mathbf{B})\hat{S}^{-1}(\mathbf{Q})(\mathbf{Q}-\mathbf{B})\right\}. \quad (8)$$

Then, substituting Eq. (7) here and integrating over directions of **Q**, we get the expression for powder-diffraction intensity:

$$J_{powder}(Q)=\frac{2\pi^2N_de^{1/2(DT^2-DL^2)}}{v_0DLDT^2Q^2\sqrt{\Delta}}\sum_{\mathbf{B}}|F(\mathbf{B})|^2\times B^{-1}\exp\left(-\frac{B^2}{2DT^2Q^2}\right)\times\{\mathrm{erf}[\sqrt{\Delta/2}(DL^{-2}\Delta^{-1}+B^2Q^{-2})]-\mathrm{erf}[\sqrt{\Delta/2}(DL^{-2}\Delta^{-1}+B^2Q^{-2})]\}, \quad (9)$$

$\Delta=DL^{-2}-DT^{-2}$.

It is evident that this equation can also describe the effect of random deformations in the process of squeezing of crystal powder. In this process there also appear random deformations of crystalline particles due to random forces exerted between them. The distributions of such forces are intensively studied in the theory of jamming granular matter[18] and some conclusive results have been obtained recently for uniaxial pressure case.[19] It was shown that possible distribution functions with varying asymmetry can be the Gaussian ones as well. Figure 7 shows the evolution of the single Bragg peak profile, in the process of crystal powder compression under nonhydrostatic conditions, described by Eq. (9). The form of spectra appears to be almost independent of the average shear deformation DT while $DT^2\leqslant DL\ll 1$. So here we choose the simple case $DT=DL\equiv D$. One can note two features of the transformation process from a narrow crystalline diffraction spot to a diffuse one: (i) considerable asymmetric peak broadening and (ii) shift of the profile maximum toward lower angles. So Eq. (9) can give reasonable (qualitative) description of the diffraction on the squeezed crystal powder.

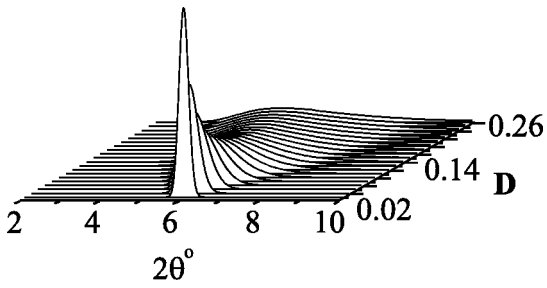

FIG. 7. Single Bragg peak profile evolution as a function of the mean-square random deformation $D=DT=DL$ (see text).

Figure 8 compares the experimentally observed diffraction patterns with the ones simulated using the structure factors of Cs_2HgBr_4 in Eq. (9). To obtain the spectrum in the experimentally accessible range of $Q=(4\pi/l)\sin\theta$ we limited the sum in Eq. (7) to **B** vectors having indexes less than 6. We also applied corrections for preferred orientation along [100] of the form $\exp(-O\varphi^2)$,[20] φ being the angle between **B** and [100] and O—an adjustable parameter. The experimentally estimated compressibility of Cs_2HgBr_4 crystal was also incorporated into the fitting procedure. From Fig. 8 one concludes that the evolution of simulated diffraction patterns corresponds sufficiently well to the observed ones, so as to lend credibility to our model of crystal amorphization by inhomogeneous deformation. If needed one could improve the fit between observed and simulated spectra by varying the size of homogeneously deformed domains (a source of additional peak broadening) and by accounting for correlated atomic displacements (peak intensity correction).

The features expected of such pseudoamorphization (amorphization without structural disordering) are those observed in Cs_2HgBr_4; namely: (i) Dissipation of long-range order produced by the mechanical deformation is a reversible process as after pressure release and stress relaxation long-range order returns. (ii) The transformation process evolves gradually and simultaneously everywhere in the sample volume, with the result that the diffraction peaks broaden without the appearance of a glass-like background in the diffraction patterns. (iii) The proposed mechanism is operative only if compression is nonhydrostatic.

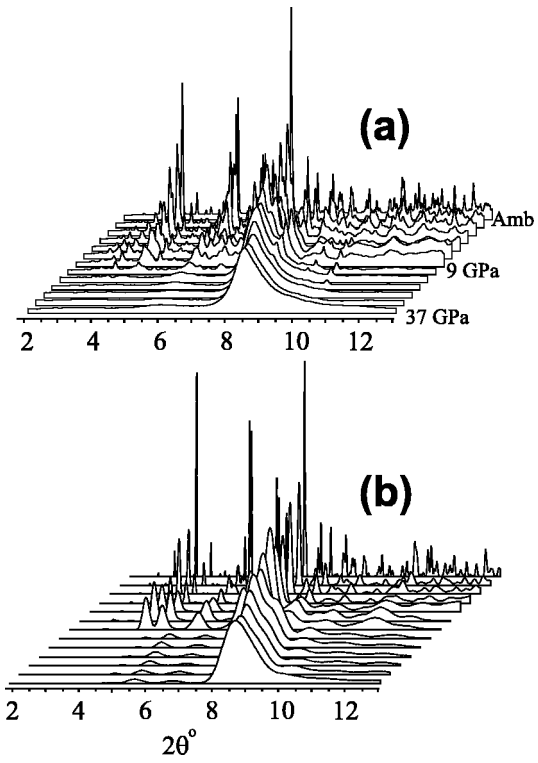

FIG. 8. Experimental diffraction patterns of Cs_2HgBr_4 collected at different pressures (a) compared with the corresponding patterns (b) simulated in the framework of the model of an inhomogeneously deformed crystal.

V. CONCLUSION AND OUTLOOK

The present study offers an explanation for pseudoamorphization, as observed in compressed Cs_2HgBr_4. The model, in its simplest form, simulates the sample heterogeneity in the form of a random distribution of homogeneously deformed crystalline domains, and employs the Gaussian-type distribution function for the amplitudes of the deformations induced in the sample by deviatoric stresses. The model does not depend to any significant degree on the short-range order in the crystal. Despite these limitations it describes sufficiently well the observed broadening of the crystal diffraction peaks and their merger into diffuse glass-like haloes as pressure increases.

Although pseudoamorphization imposes no special restrictions on the sample characteristics, it is clear that the materials possessing large compressibility are more susceptible to the effect, as this is the case for the Cs_2HgBr_4 crystal with $K_{0T}^{BM}=6.1$ GPa. However, in the low compressible compounds pseudoamorphization can be triggered at a moderate pressure by a strongly first-order structural transition. The conflict between internal stresses, induced in the sample by the transformation, and external deviatoric stresses can result into inhomogeneously distorted frustrated state devoid of a crystallinity, which seems to be the case for quartz having the bulk modulus $K_{0T}^{BM}=37.12$ GPa.[12,21] The present model is thus applicable to a larger variety of compounds than discussed in this paper.

ACKNOWLEDGMENTS

We are grateful to Dr. V. Pakhomov for providing us with the single crystals of Cs_2HgBr_4. Dr. T. Le Bihan is acknowledged for fruitful discussions. Experimental assistance from the staff of the Swiss-Norwegian Beam Lines and ID30 line at ESRF is gratefully acknowledged. The Swiss National Science foundation is thanked for its support, and Ministère de l'Education Nationale et de la Recherche Technologique for a bursary to D.M.

[1] O. Mishima, L.D. Calvert, and E. Whalley, Nature (London) **310**, 393 (1984).
[2] E.G. Ponyatovsky and O.I. Barkalov, Mater. Sci. Rep. **8**, 147 (1992).
[3] S.M. Sharma and S.K. Sikka, Prog. Mater. Sci. **40**, 1 (1996).
[4] P. Richet and P. Gillet, Eur. J. Mineral. **9**, 907 (1997).
[5] D. Altermatt, H. Arend, V. Gramlich, A. Niggli, and W. Petter, Acta Crystallogr., Sect. B: Struct. Sci. **40**, 347 (1984).
[6] A.P. Hammersley, S.O. Svensson, M. Hanfland, A.N. Fitch, and D. Hausermann, High Press. Res. **14**, 235 (1996).
[7] H.K. Mao, J. Xu, and P.M. Bell, J. Geophys. Res. **91**, 4673 (1986).
[8] A.V. Kityk, O.M. Mokry, V.P. Soprunyuk, and O.G. Vlokh, J. Phys.: Condens. Matter **5**, 5189 (1993).
[9] We keep this notation even if paraffin oil provides good hydrostaticity in that pressure range.
[10] A.V. Kityk, A.V. Zadorozhna, Ya. I. Shchur, I. Yu. Martynyuk-Lototska, Ya. Burak, and O.G. Vlokh, Aust. J. Phys. **51**, 943 (1998).
[11] G. Serghiou, H.-J. Reichmann, and R. Boehler, Phys. Rev. B **55**, 14 765 (1997).
[12] J. Haines, J.M. Léger, F. Gorelli, and M. Hanfland, Phys. Rev. Lett. **87**, 155503 (2001).
[13] V. Dmitriev, V. Sinitsyn, R. Dilanian, D. Machon, A. Kuznetsov, E. Ponyatovsky, G. Lucazeau, and H.P. Weber, J. Phys. Chem. Solids **64**, 307 (2003).
[14] N. Binggeli and J.R. Chelikowsky, Phys. Rev. Lett. **69**, 2220 (1992).
[15] N. Binggeli, J.R. Chelikowsky, and R.M. Wentzcovitch, Phys. Rev. B **49**, 9336 (1994).
[16] M.H. Cohen, J. Iñigues, and J.B. Neaton, J. Non-Cryst. Solids **307-310**, 602 (2002).
[17] P.N. Timonin, I.N. Zakharchenko, O.A. Bunina, and V.P. Sakhnenko, Phys. Rev. B **58**, 3015 (1998).
[18] P.G. de Gennes, Rev. Mod. Phys. **71**, S374 (1999).
[19] T. Aste, T. Di Matteo, and E. Galleani d'Agliano, J. Phys.: Condens. Matter **14**, 2391 (2002).
[20] *International Tables for Crystallography*, edited by A. J. C. Wilson (Kluwer, Dordrecht, 1995), Vol. C, p. 61.
[21] R.J. Angel, D.R. Allan, R. Miletich, and L.W. Finger, J. Appl. Crystallogr. **30**, 461 (1997).